

Human iPS cell-derived dopaminergic neurons function in a primate Parkinson's disease model

Tetsuhiro Kikuchi¹, Asuka Morizane¹, Daisuke Doi¹, Hiroaki Magotani¹, Hirotaka Onoe², Takuya Hayashi², Hiroshi Mizuma², Sayuki Takara², Ryosuke Takahashi³, Haruhisa Inoue⁴, Satoshi Morita⁵, Michio Yamamoto⁵, Keisuke Okita⁶, Masato Nakagawa⁶, Malin Parmar⁷ & Jun Takahashi^{1,8}

Induced pluripotent stem cells (iPS cells) are a promising source for a cell-based therapy to treat Parkinson's disease (PD), in which midbrain dopaminergic neurons progressively degenerate^{1,2}. However, long-term analysis of human iPS cell-derived dopaminergic neurons in primate PD models has never been performed to our knowledge. Here we show that human iPS cell-derived dopaminergic progenitor cells survived and functioned as midbrain dopaminergic neurons in a primate model of PD (*Macaca fascicularis*) treated with the neurotoxin MPTP. Score-based and video-recording analyses revealed an increase in spontaneous movement of the monkeys after transplantation. Histological studies showed that the mature dopaminergic neurons extended dense neurites into the host striatum; this effect was consistent regardless of whether the cells were derived from patients with PD or from healthy individuals. Cells sorted by the floor plate marker CORIN did not form any tumours in the brains for at least two years. Finally, magnetic resonance imaging and positron emission tomography were used to monitor the survival, expansion and function of the grafted cells as well as the immune response in the host brain. Thus, this preclinical study using a primate model indicates that human iPS cell-derived dopaminergic progenitors are clinically applicable for the treatment of patients with PD.

Midbrain dopaminergic neurons can be efficiently induced from human embryonic stem cells (ES cells) and iPS cells^{3–5} and, when grafted into the striatum, can improve the impaired behaviour of rat¹ and non-human primate⁶ models of PD. Cell differentiation protocols that generate clinically applicable dopaminergic neurons from human ES cells or iPS cells have been proposed recently^{1,2,4,5}. To address the efficacy and safety of the generated dopaminergic neurons, we induced dopaminergic progenitor cells and grafted them into the putamen of MPTP-treated cynomolgus monkeys. Another concern is whether dopaminergic neurons derived from patients with PD could survive and function after transplantation as well as those derived from healthy individuals^{7–10}. Therefore, we investigated the function of dopaminergic neurons derived from both patients with sporadic PD and healthy individuals.

We established eight iPS cell lines from four healthy individuals and three patients with PD (Table 1). Then, we induced midbrain dopaminergic progenitor cells through a dual SMAD inhibition and floor plate induction protocol². We isolated cells expressing CORIN (a floor plate marker in the developing brain also known as atrial natriuretic peptide-converting enzyme) on day 12 and cultured the sorted cells as floating spheres until day 28 (Extended Data Fig. 1a). The percentage of CORIN⁺ cells varied between cell lines before sorting on day 12 (Table 1, Extended Data Fig. 1b), but was greater than 90% in every cell line after sorting.

Because midbrain dopaminergic neurons are generated from neurons in the floor plate^{11,12}, we defined an effective population as cells that expressed both FOXA2 (a floor plate marker) and TUJ1 (a neuronal marker). An immunofluorescence study of cells at day 26 revealed that $87.5 \pm 2.6\%$ (mean \pm s.d.) of cells were FOXA2⁺TUJ1⁺, and $16.4 \pm 3.8\%$ expressed NURR1, a marker of midbrain dopaminergic neurons¹³ (Table 1, Extended Data Fig. 1c). There was no significant difference in the percentage of these markers between healthy individuals and patients with PD (Extended Data Fig. 1d, e). Following prolonged culture, these cells produced action potentials (Extended Data Fig. 1f) and released dopamine (272 ± 71 pg per 10^6 cells, $n = 4$) (Extended Data Fig. 1g) in response to high potassium stimulation.

Next, we examined whether the donor cells might include tumorigenic cells. On day 26, the expression levels of pluripotent cell markers (OCT4 encoded by *POU5F1*, NANOG, LIN28A) was 1% or less compared with those of undifferentiated cells (Table 1). In addition, immunostaining detected no OCT4⁺ cells in all cell lines. If neuroepithelial cells and radial glial cells remained in the donor cells, they might slowly proliferate in the brain¹⁴. But we found no or only a few SOX1⁺Ki-67⁺ and PAX6⁺Ki-67⁺ cells in the donor cells (Table 1, Extended Data Fig. 1c). Neural rosette-forming cells (SOX1⁺PAX6⁺) contribute to tumour formation, but such cells were not observed.

To investigate the efficacy and safety of the donor cells, we grafted day 28 dopaminergic progenitor cells² into the putamen of MPTP-treated monkeys on both sides. For immunosuppression, FK506 was administered daily from one day before the cell transplantation until the day of euthanasia. Blood concentration of FK506 was stable and the average trough value was 22.2 ± 12.6 ng ml⁻¹ (Extended Data Table 1). One monkey (number 10) unexpectedly weakened at eight months, owing to acute gas accumulation in the intestines, and was euthanized. We omitted this monkey from the behavioural analyses. To evaluate the neurological findings, we used two methods: a neurological rating scale (Extended Data Fig. 2a) and a video-based analysis of spontaneous movements. The monkeys that had received cell transplants showed gradual improvements in scores (Fig. 1a, Extended Data Fig. 2b). The recovery rates were significantly higher in the transplanted monkeys: 53.6 ± 8.5 , 41.7 ± 14.4 and $10.4 \pm 10.0\%$ at 12 months for the cells from healthy individuals, cells from patients with PD and control injections, respectively (Fig. 1b). There was no difference in recovery whether the donor cells were derived from healthy individuals or patients with PD. Abnormal behaviour, such as dyskinesia, was not observed. The amount of spontaneous movement was quantified on the basis of pixel changes in video frames during a 90-min period (Extended Data Fig. 2c–f). When we set the threshold at 5,000 pixels per 0.033 seconds, equivalent to the movement of a position change, a significant increase in movement was observed only in the transplanted group (Fig. 1c,

¹Department of Clinical Application, Center for iPS Cell Research and Application, Kyoto University, Kyoto 606-8507, Japan. ²Division of Bio-Function Dynamics Imaging, RIKEN Center for Life Science Technologies, Kobe 650-0047, Japan. ³Department of Neurology, Kyoto University Graduate School of Medicine, Kyoto 606-8507, Japan. ⁴Department of Cell Growth and Differentiation, Center for iPS Cell Research and Application, Kyoto University, Kyoto 606-8507, Japan. ⁵Department of Biomedical Statistics and Bioinformatics, Kyoto University Graduate School of Medicine, Kyoto 606-8507, Japan. ⁶Department of Life Science Frontiers, Center for iPS Cell Research and Application, Kyoto University, Kyoto 606-8507, Japan. ⁷Wallenberg Neuroscience Center and Lund Stem Cell Center, Lund University, 22184 Lund, Sweden. ⁸Department of Neurosurgery, Clinical Neuroscience, Graduate School of Medicine, Kyoto University, Kyoto 606-8507, Japan.

Table 1 | Characteristics of dopamine neuron progenitors

Monkey no.	Cell line	iPS cell no.	Origin	Factors	Day 12				Day 26				qPCR (relative to day 0)			
					flow cytometry		Immunohistochemistry									
					CORIN ⁺ (pre-sort) (%)	CORIN ⁺ (post-sort) (%)	FOXA2 ⁺ TUJ1 ⁺ (%)	FOXA2 ⁺ TUJ1 ⁺ (%)	NURR1 ⁺ (%)	Ki-67 ⁺ (%)	SOX1 ⁺ Ki-67 ⁺ (%)	PAX6 ⁺ Ki-67 ⁺ (%)	OCT4	NANOG	LIN28A	
2	N117-11	Healthy person no. 1 (74M), DF	4F, LIN28A, GLIS1	12.5	90.7	94.2	87.0	15.0	7.3	0.0	0.0	4.7 × 10 ⁻⁶	2.9 × 10 ⁻³	7.6 × 10 ⁻⁵		
4	1147F1	Healthy person no. 2 (50M), PBC	4F, LIN28A, shp53	15.5	90.7	91.5	90.6	12.6	5.0	0.0	0.0	1.9 × 10 ⁻⁵	4.9 × 10 ⁻²	4.1 × 10 ⁻⁴		
7	836B3	HDF1388 (36F), DF	4F, LIN28A, GLIS1	25.5	90.5	98.9	88.9	22.8	5.9	0.0	0.8	2.3 × 10 ⁻⁶	1.9 × 10 ⁻³	9.0 × 10 ⁻⁵		
11	1231A3	Healthy person no. 3 (29F), PBC	4F, LIN28A, p53DD	25.9	94.9	96.9	90.6	20.9	8.8	0.0	0.3	9.2 × 10 ⁻⁷	1.7 × 10 ⁻²	9.6 × 10 ⁻⁵		
1	PD12-1	PD patient no. 12 (52M), DF	4F, LIN28A, GLIS1	26.9	92.5	99.0	88.0	17.3	14.2	0.0	0.4	4.5 × 10 ⁻⁶	2.3 × 10 ⁻³	N.D.		
6	783E2	PD patient no. 12 (52M), PBC	4F, LIN28A, shp53	21.6	90.6	88.3	83.1	12.1	6.8	0.2	0.2	2.3 × 10 ⁻⁵	3.7 × 10 ⁻³	3.8 × 10 ⁻⁴		
9	1275A3	PD patient no. 15 (71M), PBC	4F, LIN28A, shp53	15.6	92.6	99.6	85.2	14.4	6.6	0.0	0.0	5.7 × 10 ⁻⁶	2.6 × 10 ⁻²	1.4 × 10 ⁻⁴		
10	1263A18	PD patient no. 2 (82M), PBC	4F, LIN28A, shp53	15.4	91.6	99.7	86.9	16.0	1.7	0.0	0.0	9.5 × 10 ⁻⁵	1.2 × 10 ⁻²	N.D.		

DF, dermal fibroblasts; PBC, peripheral blood cells; 4F: OCT4, SOX2, KLF4, and L-MYC. N.D., not detected. Donor age (years) and sex (M, male; F, female) in parentheses.

Extended Data Fig. 2g, h). This result was also true when we set the threshold at 10,000 pixels per 0.033 seconds, equivalent to the movement of walking (Fig. 1d, Extended Data Fig. 2i, j).

Next, we compared the efficacy of the transplantation with that of medical treatment with L-DOPA, a drug commonly used to treat PD. The extent of recovery after cell transplantation was similar in terms of neurological score and lower in terms of spontaneous movement than that produced by high dose (20 mg kg⁻¹) L-DOPA administration (Extended Data Fig. 2k, l). Given that MPTP-treated monkeys showed improvements in PD scores ranging from 15 to 33% with L-DOPA¹⁵, the transplantation of iPS cell-derived dopaminergic progenitors should exert effects similar to those of L-DOPA treatment.

To confirm the safety of the grafted cells, we monitored cell survival and proliferation by magnetic resonance imaging (MRI) and positron emission tomography (PET) for more than 12 months (and up to 24 months) after transplantation. Grafts were recognized as the hyperintensity areas in T2-weighted images, which may possibly include oedema around the grafts, cell migration or neurite extension (Fig. 2a). The calculated graft volume increased gradually until 6–9 months after transplantation, but reached a plateau thereafter (Fig. 2b). Analysis using a linear mixed effect model revealed that the estimated maximum value of the 95% confidence upper limit of graft volume at 24 months was 106.70 mm³, and the peak of the estimated average value was 50.73 mm³ at 18 months (Extended Data Fig. 3a). Histological analysis of the brain revealed that the calculated graft volumes based on STEM121 (a human cell marker) staining differed in each animal (Fig. 2c), and the average value was 39.4 ± 21.2 mm³ (*n* = 16), indicating that these grafts were unlikely to cause a mass effect. MRI-based graft volumes were consistent with those obtained by immunohistochemistry (Extended Data Fig. 3b). Haematoxylin–eosin staining showed that the grafts contained no rosette formation or malignant findings such as pleomorphism (Fig. 2d). We did not observe Ki-67⁺ proliferating cells in the grafts (Fig. 2e–g). Consistent with these findings, an [¹⁸F]fluorothymidine (FLT)-PET study, which can detect actively proliferating cells⁶, revealed no uptake of [¹⁸F]FLT in any monkey (Fig. 2h).

Histological analysis with 3,3'-diaminobenzidine (DAB) staining for tyrosine hydroxylase (TH) demonstrated survival of the grafted dopaminergic neurons. In some cases (monkeys 1, 2, 10 and 11), neurite extension covered the entire putamen and part of the caudate head (Fig. 3a–c, Extended Data Fig. 4a). High-magnification images revealed that the size and morphology of the TH⁺ cells were similar to those of host dopaminergic neurons in the substantia nigra (Fig. 3d, Extended Data Fig. 4b). Most of the surviving cells expressed FOXA2 (Fig. 3e), and 33.3 ± 24.4% of them also expressed tyrosine hydroxylase (Fig. 3f).

This relatively low maturation rate is consistent with previous observations of transplanted human ES cell- or iPS cell-derived dopaminergic progenitors in 6-hydroxydopamine-lesioned rat models, in which 6–54% of surviving cells expressed tyrosine hydroxylase at 16–18 weeks after transplantation^{1,2,5}. The average number of these TH⁺

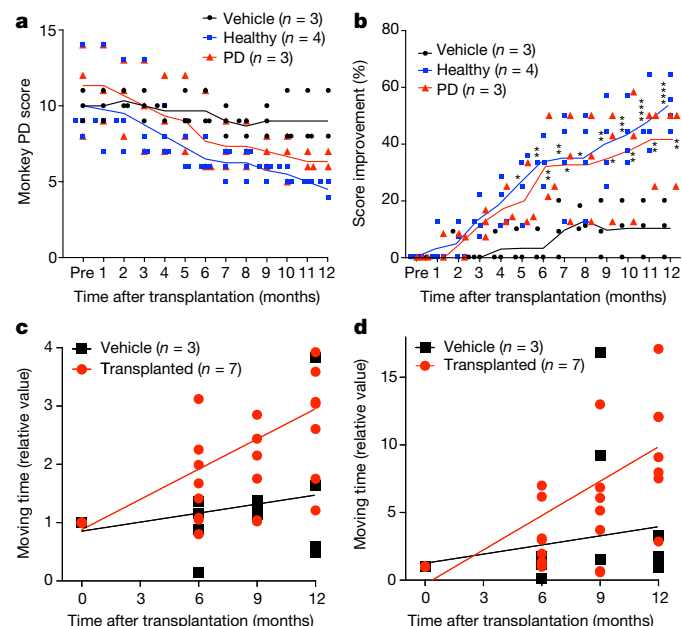


Figure 1 | Behavioural analysis of monkeys. **a, b**, Neurological scores (a) and score improvements (b) of the monkeys. Vehicle, monkeys that received control injections of vehicle; PD, monkeys transplanted with cells derived from patients with PD; Healthy, monkeys transplanted with cells derived from healthy individuals. Lines show mean values (*n* = 3 for vehicle and PD groups, 4 for healthy group). Two-way analysis of variance (ANOVA) with Dunnett's multiple comparisons test was performed; **P* < 0.05; ***P* < 0.01; ****P* < 0.001; *****P* < 0.0001 versus vehicle group. **c, d**, Linear regression analysis of moving time of monkeys analysed by video recordings when the threshold was set to 5,000 (c) or 10,000 (d) pixels per 0.033 seconds. Values are shown relative to each pre-operative value, which was set to 1 (*n* = 3 for vehicle group, 7 for transplanted group). The *P* and *r*² values and regression equations are 0.0016, 0.33 and $y = 0.17x + 0.88$ (c, transplanted), 0.44, 0.067 and $y = 0.052x + 0.85$ (c, vehicle), 0.0007, 0.37 and $y = 0.85x - 0.31$ (d, transplanted) and 0.18, 0.051 and $y = 0.23x + 1.3$ (d, vehicle), respectively. All Source Data for the graphs are provided with the online version of the paper.

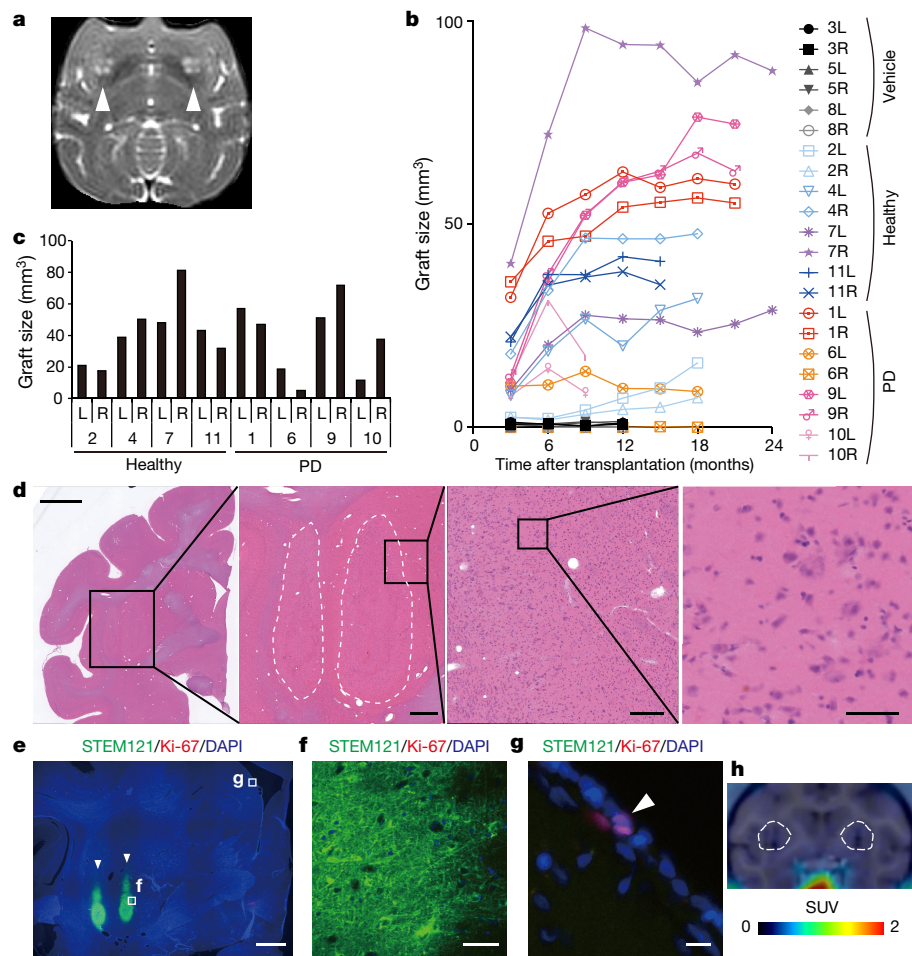


Figure 2 | Growth and survival of iPS cell-derived dopaminergic neuron progenitors *in vivo*. **a**, Representative MRI of a cell-transplanted monkey (number 11, 12 months after transplantation). Arrowheads indicate grafts. **b**, Graft sizes estimated from MRI. **c**, Graft sizes at the time of euthanasia. **d**, Representative haematoxylin-eosin staining of brain tissue from monkey 1. The box in each image outlines the area magnified to the right.

Dotted white lines designate the graft. Scale bars, 5 mm, 1 mm, 200 μm and 50 μm from left to right. **e**, Representative image of double staining for STEM121 and Ki-67⁺. **f**, **g**, Magnified view of the graft (**f**) and ventricular wall (**g**, positive control) in **e**. Scale bars, 2 mm (**e**), 50 μm (**f**) and 10 μm (**g**). **h**, A representative image obtained by $[^{18}\text{F}]$ FLT-PET. Dotted white lines designate the putamen.

dopaminergic neurons was $6.4 \pm 4.9 \times 10^4$ per hemisphere (Fig. 3f), with no difference between grafts derived from healthy individuals or patients with PD ($5.4 \pm 4.7 \times 10^4$ and $7.3 \pm 5.3 \times 10^4$, respectively). These TH⁺ cells also expressed midbrain dopaminergic neuron markers such as dopamine transporter (DAT) (Fig. 3g), and a marker for A9-type dopaminergic neurons of the nigrostriatal pathway, GIRK2 (Fig. 3h). Because cell sorting by CORIN eliminates serotonergic neurons², we found no serotonin⁺ cells in the grafts. We found few (less than 1%) GABA⁺ or GFAP⁺ cells and no VGLUT1⁺ or CHAT⁺ cells. Finally, we observed no specific pathological findings, such as Lewy bodies, even in grafts derived from patients with PD.

To determine whether the grafted cells functioned as dopaminergic neurons, we examined dopamine synthesis by $[^{18}\text{F}]$ DOPA-PET⁶ and found a gradual increase in $[^{18}\text{F}]$ DOPA uptake in the putamen (Fig. 3i–k). The average influx constant (K_i) values of normal monkeys, MPTP-treated monkeys and those with transplantation were 7.1 ± 0.18 ($n = 2$), 0.84 ± 0.60 ($n = 11$), and 3.5 ± 1.9 ($n = 7$), respectively, indicating that the K_i values of transplanted monkeys recovered to about 48% of the levels found in normal monkeys. The K_i values significantly correlated with the number of surviving TH⁺ cells in the grafts ($r = 0.56$, $P = 0.022$), suggesting that the survival of dopaminergic neurons can be monitored by $[^{18}\text{F}]$ DOPA-PET (Fig. 3l). As another indicator, we also examined DAT expression by $[^{11}\text{C}]$ PE2I-PET¹⁶. Although DAT⁺ cells were observed in six monkeys (numbers 1, 6, 7, 9, 10 and 11), an apparent increase in the binding potential of

$[^{11}\text{C}]$ PE2I was detected in only two monkeys (numbers 1 and 10; Fig. 3g, Extended Data Fig. 5a–c).

To estimate the effective range of the grafted cells, we analysed the relationship between the degree of behavioural recovery and the number of surviving TH⁺ cells (Extended Data Fig. 6a, b) or the area innervated by TH⁺ fibres (Extended Data Fig. 6c, d). Even the lowest number of surviving TH⁺ cells (16,000 cells) and the smallest innervation area (9.3%) exerted a saturating effect. The impaired behaviour of MPTP-treated monkeys can be restored by the transplantation of dopaminergic neurons derived from monkey ES cells¹⁷, monkey iPS cells¹⁸ and human ES cells⁶, in which 4,300–13,000 TH⁺ cells survived per animal. In the clinical cases of transplantation of fetal ventral mesencephalon cells into patients with PD, 43,000–240,000 TH⁺ cells were observed after death in the brains of patients whose symptoms had improved^{19–22}. Given that the volume ratio between human and cynomolgus monkey putamens is 6.55:1 (ref. 23), 16,000 TH⁺ cells in monkeys is equivalent to about 100,000 TH⁺ cells in humans, and the result of this study is reasonable. In addition, transplantation of human fetal ventral mesencephalon cells into monkey PD models showed a 40–60% improvement in PD scores²⁴, while we found a 40–55% improvement in the present study (Fig. 1b, Extended Data Fig. 6a, c). These results suggest that iPS cell-derived dopaminergic neurons will exert an effect similar to that of human fetal ventral mesencephalon cells.

The immune response by the host brain was monitored by two PET studies (Extended Data Fig. 7a). One of the ligands used, $[^{11}\text{C}]$ PK11195

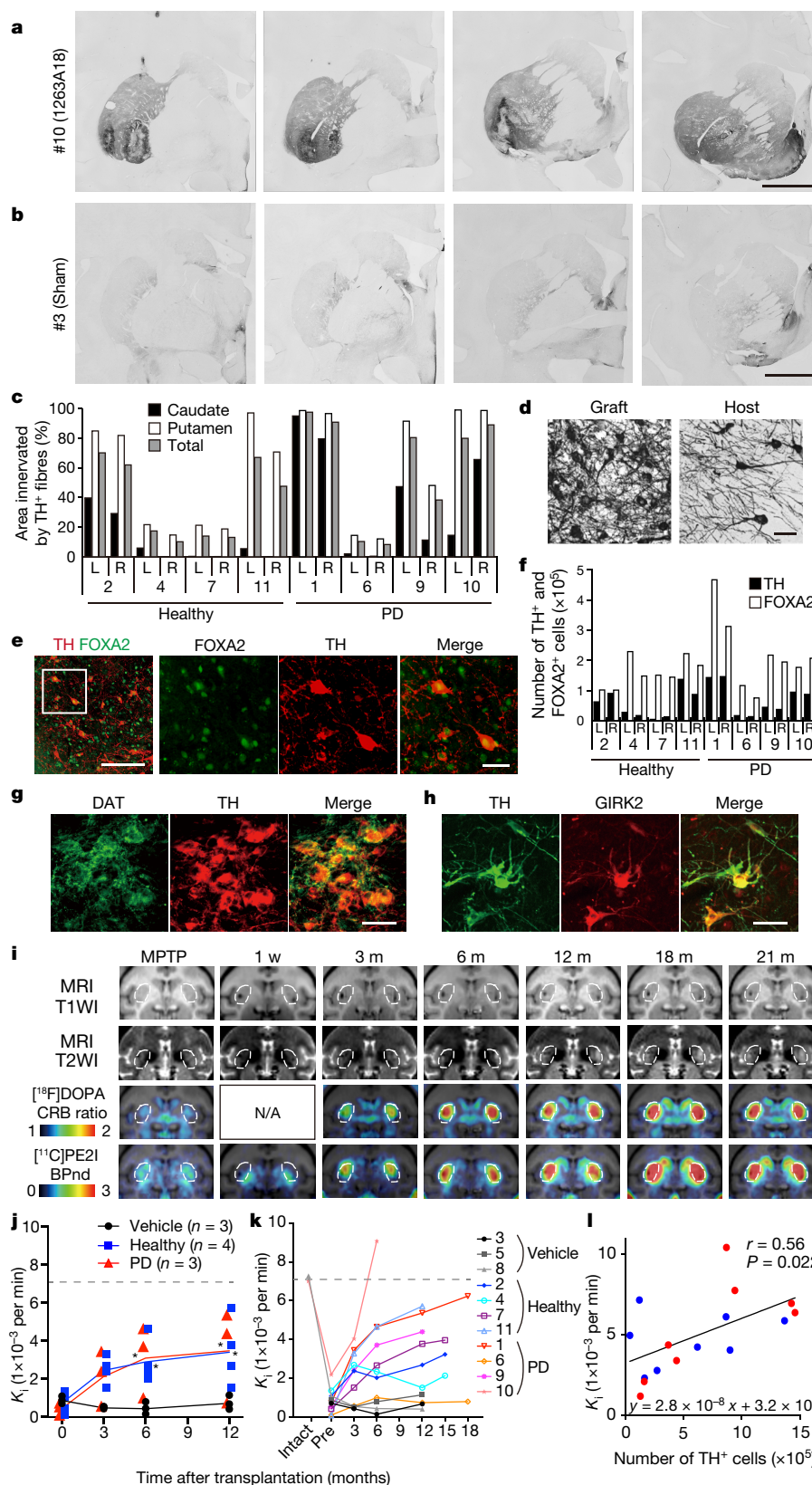


Figure 3 | Characteristics of surviving TH⁺ cells. **a, b**, Successive images of tyrosine hydroxylase staining of monkeys 10 (PD group, **a**) and 3 (vehicle group, **b**). Scale bars, 5 mm. **c**, Percentage of area in which TH⁺ fibres are innervated in caudate nuclei, putamen, and whole striatum of each monkey. **d**, Magnified view of TH⁺ neurons in the graft (left) and substantia nigra (right). Scale bar, 50 μ m. **e**, Representative immunostaining images for FOXA2 and tyrosine hydroxylase. Scale bars, 200 μ m (left image) and 50 μ m (three images to the right). **f**, The number of TH⁺ cells and FOXA2⁺ cells surviving in each monkey. **g, h**, Representative images of double staining for DAT and G-protein-activated inward rectifier potassium channel 2 (GIRK2). **i**, Time course of MRI and PET of a representative monkey (number 1). Dotted white lines designate the putamen. m, months; w, weeks. **j**, K_i values obtained from [¹⁸F]DOPA-PET. Lines show mean values ($n = 3$ for vehicle and PD groups, 4 for healthy group). Two-way ANOVA with Dunnett's multiple comparisons test was performed. * $P < 0.05$ versus vehicle group. **k**, K_i values obtained from [¹⁸F]DOPA-PET in each monkey. Dotted lines in **j** and **k** designate the average K_i value for two intact monkeys. **l**, Correlation between surviving TH⁺ cells and K_i values from [¹⁸F]DOPA-PET. Two-tailed Pearson's correlation analysis was performed, and r and P values are shown. A linear regression line is also shown. Data for the healthy group are shown in blue, and the PD group in red.

(ref. 25), binds to a translocator protein expressed by activated microglia. The other, S-[¹¹C]KTP-Me (ref. 26), is expressed on microglia in the inflammatory brain. Both PET studies showed no change in the uptake of these ligands (Extended Data Fig. 7b, c). To evaluate indirect xenorecognition through host-derived antigen-presenting cells, we performed immunofluorescence staining for major histocompatibility complex (MHC) class II antigens expressed by activated microglia,

Although monkeys with patient-derived dopaminergic progenitors had a large number of MHC class II⁺ cells, no or only few CD45⁺ leukocytes and IgG deposits accumulated even in these monkeys (Extended Data Fig. 7d, 8). These results suggest that no or only a very mild immune response was elicited under a sufficient dose of immunosuppressant.

The number of surviving dopaminergic neurons differed between monkeys, suggesting that unknown characteristics that vary between

cell lines may affect cell survival or differentiation. To identify these characteristics, we examined the gene expression profiles of the remnants of the donor cells used for transplantation. A principal component analysis revealed that all donor cells formed a cluster close to the fetal midbrain, but distinct from undifferentiated iPS cells or the human adult substantia nigra (Extended Data Fig. 9a).

In this study, we randomly chose one cell line from each donor. In a clinical situation, however, only the best cell lines would be considered, which should reduce the variability of graft survival and graft outcome. For this purpose, indicators of good donor cells would be helpful. To address this issue, we divided the monkeys into excellent and relatively poor groups in terms of the number of surviving TH⁺ cells, the areas innervated by TH⁺ fibres and [¹⁸F]DOPA-PET. A microarray analysis between the two groups (numbers 1 and 10 versus numbers 4 and 6) resulted in the identification of 11 genes that were upregulated in the excellent group (Extended Data Fig. 9b, c). Recently, a global gene expression analysis of human ES cell-derived dopaminergic progenitors grafted into rat PD models reported markers of donor cells that were predictive of a good outcome after transplantation²⁷. Notably, that analysis and ours found a common candidate gene, *Dlk1* (Extended Data Fig. 9b). *Dlk1* belongs to an epidermal growth factor superfamily²⁸. In the murine brain, its expression can be detected as early as embryonic day 11.5 in the ventral mesencephalon and overlaps that of tyrosine hydroxylase^{29,30}, suggesting that *Dlk1* plays an important role in the differentiation of midbrain dopaminergic neurons²⁸. Further investigation will be needed to confirm whether *Dlk1* might be a predictive marker of good donor cells.

In conclusion, these results will contribute to the development of translational medical techniques that use pluripotent stem cells to treat intractable neurological diseases.

Online Content Methods, along with any additional Extended Data display items and Source Data, are available in the online version of the paper; references unique to these sections appear only in the online paper.

Received 24 November 2016; accepted 19 July 2017.

- Kriks, S. et al. Dopamine neurons derived from human ES cells efficiently engraft in animal models of Parkinson's disease. *Nature* **480**, 547–551 (2011).
- Doi, D. et al. Isolation of human induced pluripotent stem cell-derived dopaminergic progenitors by cell sorting for successful transplantation. *Stem Cell Reports* **2**, 337–350 (2014).
- Perrier, A. L. et al. Derivation of midbrain dopamine neurons from human embryonic stem cells. *Proc. Natl Acad. Sci. USA* **101**, 12543–12548 (2004).
- Chambers, S. M. et al. Highly efficient neural conversion of human ES and iPS cells by dual inhibition of SMAD signaling. *Nat. Biotechnol.* **27**, 275–280 (2009).
- Kirkeby, A. et al. Generation of regionally specified neural progenitors and functional neurons from human embryonic stem cells under defined conditions. *Cell Reports* **1**, 703–714 (2012).
- Doi, D. et al. Prolonged maturation culture favors a reduction in the tumorigenicity and the dopaminergic function of human ESC-derived neural cells in a primate model of Parkinson's disease. *Stem Cells* **30**, 935–945 (2012).
- Hargus, G. et al. Differentiated Parkinson patient-derived induced pluripotent stem cells grow in the adult rodent brain and reduce motor asymmetry in Parkinsonian rats. *Proc. Natl Acad. Sci. USA* **107**, 15921–15926 (2010).
- Nguyen, H. N. et al. LRRK2 mutant iPSC-derived DA neurons demonstrate increased susceptibility to oxidative stress. *Cell Stem Cell* **8**, 267–280 (2011).
- Sánchez-Danés, A. et al. Disease-specific phenotypes in dopamine neurons from human iPS-based models of genetic and sporadic Parkinson's disease. *EMBO Mol. Med.* **4**, 380–395 (2012).
- Kikuchi, T. et al. Idiopathic Parkinson's disease patient-derived induced pluripotent stem cells function as midbrain dopaminergic neurons in rodent brains. *J. Neurosci. Res.* **95**, 1829–1837 (2017).
- Ono, Y. et al. Differences in neurogenic potential in floor plate cells along an anteroposterior location: midbrain dopaminergic neurons originate from mesencephalic floor plate cells. *Development* **134**, 3213–3225 (2007).
- Joksimovic, M. et al. Wnt antagonism of *Shh* facilitates midbrain floor plate neurogenesis. *Nat. Neurosci.* **12**, 125–131 (2009).
- Smidt, M. P. et al. A homeodomain gene *Ptx3* has highly restricted brain expression in mesencephalic dopaminergic neurons. *Proc. Natl Acad. Sci. USA* **94**, 13305–13310 (1997).
- Katsukawa, M., Nakajima, Y., Fukumoto, A., Doi, D. & Takahashi, J. Fail-safe therapy by gamma-ray irradiation against tumor formation by human-induced pluripotent stem cell-derived neural progenitors. *Stem Cells Dev.* **25**, 815–825 (2016).

- Imbert, C., Bezard, E., Guitraud, S., Boraud, T. & Gross, C. E. Comparison of eight clinical rating scales used for the assessment of MPTP-induced parkinsonism in the Macaque monkey. *J. Neurosci. Methods* **96**, 71–76 (2000).
- Kikuchi, T. et al. Survival of human induced pluripotent stem cell-derived midbrain dopaminergic neurons in the brain of a primate model of Parkinson's disease. *J. Parkinsons Dis.* **1**, 395–412 (2011).
- Takagi, Y. et al. Dopaminergic neurons generated from monkey embryonic stem cells function in a Parkinson primate model. *J. Clin. Invest.* **115**, 102–109 (2005).
- Hallett, P. J. et al. Successful function of autologous iPSC-derived dopamine neurons following transplantation in a non-human primate model of Parkinson's disease. *Cell Stem Cell* **16**, 269–274 (2015).
- Freed, C. R. et al. Transplantation of embryonic dopamine neurons for severe Parkinson's disease. *N. Engl. J. Med.* **344**, 710–719 (2001).
- Olanow, C. W. et al. A double-blind controlled trial of bilateral fetal nigral transplantation in Parkinson's disease. *Ann. Neurol.* **54**, 403–414 (2003).
- Kurowska, Z. et al. Signs of degeneration in 12–22-year old grafts of mesencephalic dopamine neurons in patients with Parkinson's disease. *J. Parkinsons Dis.* **1**, 83–92 (2011).
- Li, W. et al. Extensive graft-derived dopaminergic innervation is maintained 24 years after transplantation in the degenerating parkinsonian brain. *Proc. Natl Acad. Sci. USA* **113**, 6544–6549 (2016).
- Yin, D. et al. Striatal volume differences between non-human and human primates. *J. Neurosci. Methods* **176**, 200–205 (2009).
- Redmond, D. E. Jr, Vinuela, A., Kordower, J. H. & Isaacson, O. Influence of cell preparation and target location on the behavioral recovery after striatal transplantation of fetal dopaminergic neurons in a primate model of Parkinson's disease. *Neurobiol. Dis.* **29**, 103–116 (2008).
- Turkheimer, F. E. et al. Reference and target region modeling of [¹¹C]-(*R*)-PK11195 brain studies. *J. Nucl. Med.* **48**, 158–167 (2007).
- Shukuri, M. et al. *In vivo* expression of cyclooxygenase-1 in activated microglia and macrophages during neuroinflammation visualized by PET with ¹¹C-ketoprofen methyl ester. *J. Nucl. Med.* **52**, 1094–1101 (2011).
- Kirkeby, A. et al. Predictive markers guide differentiation to improve graft outcome in clinical translation of hESC-based therapy for Parkinson's disease. *Cell Stem Cell* **20**, 135–148 (2017).
- Liechti, R. et al. Characterization of fetal antigen 1/delta-like 1 homologue expressing cells in the rat nigrostriatal system: effects of a unilateral 6-hydroxydopamine lesion. *PLoS ONE* **10**, e0116088 (2015).
- Christophersen, N. S. et al. Midbrain expression of Delta-like 1 homologue is regulated by GDNF and is associated with dopaminergic differentiation. *Exp. Neurol.* **204**, 791–801 (2007).
- Bauer, G. et al. *In vivo* biosafety model to assess the risk of adverse events from retroviral and lentiviral vectors. *Mol. Ther.* **16**, 1308–1315 (2008).

Supplementary Information is available in the online version of the paper.

Acknowledgements We thank K. Sekiguchi, J. Toga and E. Yagi for providing recombinant LM511-E8, Y. Ono for anti-CORIN and anti-NURR1 antibodies, H. Doi, A. Mawatari, M. Tsuji, K. Takahashi, M. Goto, Y. Wada, A. Yamazaki, T. Kawasaki, C. Takeda, N. Shibata, S. Kurai, A. Iglesaka, T. Mori, R. Zochi, E. Hayashinaka, M. Yamano, T. Ose, M. Ohno and K. Onoe for supporting the PET study, H. Ohmori for an electrophysiological study, S. Nolbrant for discussions about gene expression by the donor cells, and Astellas Pharma Inc. for FK506. We also thank P. Karagiannis for reading of the manuscript, K. Kubota, Y. Ishii, Y. Morita and Y. Katano for technical assistance, K. Nishimura, M. Motono, Y. Ioroi, B. Samata, Y. Koshiba, Y. Nakajima and Y. Miyawaki for taking care of the animals, and S. Tsuji, J. Mitsui and S. Morishita for whole-exome analysis of patients with PD. This study was supported by grants from the Highway Project for Realization of Regenerative Medicine from the Ministry of Education, Culture, Sports, Science and Technology (MEXT), the Network Program for Realization of Regenerative Medicine from the Japan Agency for Medical Research and Development (AMED) and the Program for Intractable Diseases Research using disease-specific iPS cells from AMED (to H.I.). M.P. is a New York Stem Cell Foundation - Robertson Investigator.

Author Contributions T.K. designed the study, performed the culture, transplantation, MRI study, data analysis and interpretation, and wrote the manuscript. A.M. and D.D. assisted with cell culture, cell sorting, transplantation and the MRI study. H.Ma. generated the PD model monkeys and performed the behavioural analysis. H.O., T.H., H.Mi. and S.T. performed the PET imaging and corresponding analysis and interpretation. R.T., H.I., K.O. and M.N. generated the iPS cells. S.M. and M.Y. performed statistical analyses. M.P. provided fetal mesencephalic samples and discussed the gene expression analyses. J.T. conceived and designed the study, assembled the data, carried out the data analysis and interpretation, wrote the manuscript, and gave final approval of the manuscript.

Author Information Reprints and permissions information is available at www.nature.com/reprints. The authors declare no competing financial interests. Readers are welcome to comment on the online version of the paper. Publisher's note: Springer Nature remains neutral with regard to jurisdictional claims in published maps and institutional affiliations. Correspondence and requests for materials should be addressed to J.T. (jbtaka@cira.kyoto-u.ac.jp).

Reviewer Information *Nature* thanks R. Barker, A. Björklund and F. Gage for their contribution to the peer review of this work.

METHODS

Generation of human iPS cells. This study was approved by the ethics committees of Kyoto University, Kyoto, Japan. iPS cells from healthy donors and patients with PD (PDiPS cells) were generated using episomal vectors as previously reported^{10,31}. The origins of the iPS cells and transduced genes are summarized in Table 1. Informed consent was obtained from all individuals. Cells that had normal karyotypes (46, XX or 46, XY) and no mycoplasma contamination were used for the experiments. Three patients with PD, PD2 (82-year-old male, PD onset at 70 years old, Hoehn & Yahr scale II), PD12 (52-year-old male, PD onset at 38 years old, Hoehn & Yahr scale III), and PD15 (71-year-old male, PD onset at 68 years old, Hoehn & Yahr scale III), without familial history of PD, were included in this study. Whole-exome analyses of these three patients were performed at the Medical Genome Center in the University of Tokyo Hospital, and we did not detect any mutations in the following PD-related genes: ACTB, ATP1A2, ATP1A3, ATP7B, DCAF17, CHMP2B, DCTN1, DRD2, FMR1, FTL, GBA, GCH1, GRN, HTRA2, HTT, JPH3, LRRK2, MAPT, NKX2-1, NUP62, PANK2, PRKN, PINK1, PLA2G6, PNKD, PRKRA, SGCE, SLC2A1, SLTRK1, SNCA, SPR, TAF1, TH, TIMM8A, TOR1A, UCHL1, VPS13A and XK.

Human iPS cell culture. Human iPS cells were initially maintained on SNL feeder layers in DMEM/F-12 (Sigma-Aldrich) supplemented with 0.1 mM 2-mercaptoethanol (Wako Pure Chemicals Industries), 20% knockout serum replacement (KSR; Invitrogen), 0.1 mM non-essential amino acids (Invitrogen), 2 mM L-glutamine, and 5 ng ml⁻¹ basic fibroblast growth factor (bFGF; Invitrogen) and expanded on E8 fragments of human laminin 511 (LM511-E8)^{32,33}. When passaging the cells to LM511-E8-coated dishes, the iPS cells were dissociated into single cells with TrypLE select (Invitrogen) and replated at a density of 1.5×10^4 cells per 6-well plate with StemFit medium (Ajinomoto). After they were passaged three times on LM511-E8 to remove feeder cells, the iPS cells were used for experiments.

Induction of dopaminergic progenitors from human iPS cells. Human iPS cells were dissociated into single cells after 10 min of incubation with TrypLE select and were plated onto LM511-E8-coated 6-well plates at a density of 4×10^5 cells per well. After 4 days of culture, the iPS cells reached a confluent state, and maintenance medium (the StemFit medium) was changed to differentiation medium containing GMEM supplemented with 8% KSR, 0.1 mM MEM non-essential amino acids (all Invitrogen), 1 mM sodium pyruvate (Sigma-Aldrich), and 0.1 mM 2-mercaptoethanol. We added 100 nM LDN193189 (Stemgent) and 500 nM A83-01 (Wako) to efficiently induce neuronal differentiation³⁴. We also added 2 μM purmorphamine and 100 ng ml⁻¹ FGF8 (Wako) from day 1 to day 7, and 3 μM CHIR99021 (Wako/Stemgent) from day 3 to day 12 to induce floor plate cells¹. After cell sorting on culture day 12, the sorted cells were replated on low cell adhesion 96-well plates (Lipidure-Coat Plate A-96U; NOF Corporation) at a density of 2×10^4 cells per well in neural differentiation medium containing neurobasal medium supplemented with B27 supplement, 2 mM L-glutamine (all Invitrogen), 10 ng ml⁻¹ GDNF, 200 mM ascorbic acid, 20 ng ml⁻¹ BDNF (all Wako), and 400 μM dbcAMP (Sigma-Aldrich). We added 30 μM Y-27632 (Wako) to the first medium to avoid apoptosis at the initial plating. After that, we changed the medium every 3 days. For prolonged culture for *in vitro* studies (Extended Data Fig. 1f, g), floating spheres were dissociated with papain and replated on plates coated with poly-L-ornithine, fibronectin, and laminin (O/F/L) at day 28 and were cultured in the neural differentiation medium until day 70.

Cell sorting. For the analysis, cells were collected using Accumax, gently dissociated into a single-cell suspension, and resuspended in phenol-free, Ca²⁺/Mg²⁺-free Hank's balanced salt solution (HBSS; Invitrogen) containing 2% FBS, 10 μM Y-27632 (Wako), 20 mM D-glucose (Wako), and 50 μg ml⁻¹ penicillin/streptomycin (Invitrogen). Samples were filtered through cell-strainer caps (35 μm mesh; BD Biosciences) and then subjected to surface marker staining using an anti-CORIN antibody (1:200; a gift from the KAN Research Institute) and Alexa 488-conjugated anti-mouse IgM antibodies (1:400; Invitrogen). The antibodies were added and the cells incubated at 4 °C for 20 min, and then the cells were washed twice with HBSS buffer. Dead cells and debris were excluded by 7-AAD staining. The analysis was performed using a FACSAria II or III cell sorter and the FACSDiva software program (BD Biosciences). A 100 μm-ceramic nozzle (BD Biosciences) with a sheath pressure of 20–25 psi and an acquisition rate of 3,000–5,000 events per second was used for sorting. Positive staining was set so that less than 0.1% of events exceeded the threshold in samples lacking primary antibodies. The sorted cells were collected and replated in U-shaped 96-well plates (Lipidure-Coat Plate A-96U; 2×10^4 cells per well) with culture medium containing 30 μM Y-27632.

Electrophysiological analysis. Whole-cell patch-clamp recordings were performed on 70-day cultured neurons grown on O/F/L-coated glass coverslips. Neurons with a large cell body and neurite-like structures were chosen for examination. The cells were maintained in a physiological saline solution of the following composition:

125 mM NaCl, 2.5 mM KCl, 2 mM CaCl₂, 1 mM MgCl₂, 26 mM NaHCO₃, 1.25 mM Na₂PO₄, and 17 mM glucose. Patch pipettes were made from borosilicate glass capillaries (GC150TF-10; Clark) and had a resistance of 3–4 MΩ when filled with an internal solution composed of 140 mM KCl, 10 mM HEPES, and 0.2 mM EGTA (pH 7.3). Recordings with a voltage clamp and current clamp were made with a patch-clamp amplifier (EPC-8; HEKA). The giga-seal resistances were in the range of 10–20 GΩ. The current signals from the amplifier were filtered at 5 kHz through a four-pole low-pass filter with Bessel characteristics (UF-BL2, NF), sampled with a 12-bit A/D converter, and stored on a 32-bit computer (PC-9821Ra333, NEC). All experiments were performed at room temperature.

PD model monkeys. Adult (2–3 years-old) male cynomolgus monkeys (*Macaca fascicularis*) were obtained from Shin Nippon Biomedical Laboratories (Kagoshima, Japan) and used for this study. The monkeys were cared for and handled according to the Guidelines for Animal Experiments of Kyoto University and the Guide for the Care and Use of Laboratory Animals of the Institute of Laboratory Animal Resources (Washington DC, USA). Monkeys were screened by spontaneous movement calculated with the PrimateScan image analysis system (CleverSys Inc.), which can calculate animal movement from analogue video. Eleven monkeys out of 38, with spontaneous movements of 100–400 movements per hour, were used in this study. To create Parkinsonian models, the animals were injected intravenously with MPTP hydrochloride (0.4 mg kg⁻¹ as a free base; Sigma-Aldrich) twice a week until we observed persistent Parkinsonian symptoms, such as tremor, bradykinesia, and impaired balance. Stable Parkinsonian symptoms were observed for more than 12 weeks before an animal was used for the experiments.

Cell transplantation. The 11 PD model monkeys were assigned into three groups (healthy, PD and vehicle group) so that the average monkey PD scores in each group were similar. We used no statistical method to determine the sample size and no randomization to allocate animals to each group. Monkeys of the healthy group (numbers 2, 4, 7 and 11) were transplanted with dopaminergic neuron progenitors derived from healthy iPS cells, and monkeys of the PD group (numbers 1, 6, 9 and 10) were transplanted with dopaminergic neuron progenitors derived from PDiPS cells. The cell lines transplanted into each monkey are described in Table 1. Monkeys of the vehicle group (numbers 3, 5 and 8) were injected with vehicle only. The coordinates of the targets were obtained using MRI, and human iPS cell-derived dopaminergic neuron progenitors were stereotactically transplanted into the putamen of the MPTP-treated monkeys bilaterally. The sphere suspension was prepared at 2×10^5 cells per μl, and 1 μl of this suspension was injected along four tracts per side (three injection sites per tract; 4.8×10^6 cells per animal). After surgery, monkeys were given antibiotics for 3 days. A daily intramuscular immunosuppressant (FK506, 0.05 mg kg⁻¹; Astellas) was given from one day before the cell transplantation until the day of euthanasia. Observation periods for each monkey were as follows: 8 months for number 10, 12 months for numbers 3, 5, 8 and 9, 15 months for number 11, 18 months for numbers 2, 4 and 6, 21 months for numbers 1 and 9, and 24 months for number 7.

MRI scans. The monkeys were subjected to MRI study before and immediately after transplantation, and once every 3 months thereafter. Animals were anaesthetized with ketamine (8 mg kg⁻¹) and xylazine (1 mg kg⁻¹), and then T1- and T2-weighted MR images were obtained using a 3-tesla MRI scanner (MAGNETOM Verio, Siemens Healthcare). Before transplantation, a high-resolution 3D T1-weighted image was obtained for each animal by a magnetization prepared rapid gradient echo (MPRAGE) sequence (TR = 2,300 ms, TE = 3.13 ms, TI = 900 ms, FA = 7°, matrix = 128 × 128, FOV, field of view = 102 mm, slice thickness = 0.8 mm) to be used for identifying the injection site (postero-dorsal striatum) of the grafts. A high-resolution 3D T2-weighted image was obtained with T2 SPACE sequence (TR = 2,500 ms, TE = 301 ms, base resolution = 128, FOV = 102 mm, slice thickness = 0.8 mm, turbo factor = 77, slice turbo factor = 2). After transplantation, in addition to T1- and T2-weighted images, a fluid-attenuated-inversion recovery (FLAIR) image (TR = 11,500 ms, TR = 81 ms, TI = 2,670.4 ms, base resolution = 128, flip angle = 150°, FOV = 102 mm, slice thickness = 0.8 mm) was also obtained to evaluate brain pathology.

MRI analysis. To calculate the graft volumes, we used Functional Magnetic Resonance Images of Brain (FMRIB) software libraries³⁵. We extracted brain images from T1- and T2-weighted images with Brain Extraction Tool³⁶, resampled them to 0.3 × 0.3 × 0.3 mm voxels in order to reduce the round-off error, and registered the T1- and T2-weighted images with FMRIB's Linear Registration Tool^{37,38}. To increase the contrast of the grafts and to remove image inhomogeneity, we created a T1w/T2w image by dividing the T1-weighted image by the T2-weighted image. Using the T1w/T2w image, the brain region was automatically segmented into four segments—grey matter, white matter, cerebrospinal fluid, and graft—using FMRIB's Automated Segmentation Tool³⁹. We manually edited the graft region when needed by careful visual inspection of other modalities of images

(FLAIR, T1w, T2w). The volume of the graft segment was calculated and assumed to represent the graft volume. The T1w/T2w images were linearly registered to the standardized MNI space of *Macaca fascicularis* for visual presentation⁴⁰.

Estimation of graft growth. The growth curves of graft sizes were estimated using the linear mixed-effects model

$$y_{ij} = \beta_0 + \beta_1 \times t_j + (\beta_2 + \alpha_{2i}) \times (t_j / (t_j + k)) + r_{ij}$$

where y_{ij} is the graft size of the i th subject at the j th time point t_j , k is the time at which the graft size reached a half of the plateau, and r_{ij} is the residual⁴¹. We estimated two grafts for each monkey (L and R) independently, so that there were 16 independent subjects. The value of k was chosen to be 7 according to Bayesian information criterion. The model contains four coefficients: three fixed effects, β_0 , β_1 , and β_2 , and a random effect, α_{2i} . Within-subject variability in repeated measures was modelled as a first-order autoregressive structure. After fitting the above model, the upper limits of the 95% confidence intervals of the predicted graft sizes were calculated for each subject using the estimated parameters.

PET study. To monitor the immunorejection and dopaminergic function in monkey brains transplanted with iPS cell-derived dopaminergic cells, *in vivo* PET imaging was performed before, 2 weeks and 1, 3, 6, 12, 18, and 24 months after, cell transplantation. Imaged monkeys were initially sedated by intramuscular injection of ketamine (10 mg kg⁻¹) and atropine (0.08 mg kg⁻¹). A plastic catheter (24G) was inserted into the inferior limbic vein through which propofol (10 mg kg⁻¹ h⁻¹) was continuously infused intravenously to achieve stable anaesthesia. The animals were placed on the gantry of an animal PET scanner (microPET Focus-220; Siemens Preclinical Solution) and were carefully monitored for physiological parameters (electrocardiograph, heart rate, SpO₂, and body temperature) throughout the PET scan. A 30-min transmission scan was performed using a ⁶⁸Ge–⁶⁸Ga pin source for attenuation correction, followed by an emission scan, which started simultaneously with the intravenous injection of a PET tracer ([¹¹C]PK11195, S-[¹¹C]KTP-Me, [¹⁸F]FLT, [¹⁸F]DOPA or [¹¹C]PE2I, 37 MBq kg⁻¹). The duration of the emission scan was 90 min for [¹¹C]PK11195, S-[¹¹C]KTP-Me, [¹⁸F]FLT, and [¹¹C]PE2I, and 120 min for [¹⁸F]DOPA. To inhibit the metabolism of [¹⁸F]DOPA to [¹⁸F]fluoro-dopamine in the peripheral tissues, carbidopa (10 mg kg⁻¹) was intravenously injected approximately 1 min before the injection of [¹⁸F]DOPA. The emission data were reconstructed using a filtered back-projection algorithm with an attenuation correction and no scatter correction. The regions of interest (ROIs) were manually drawn on the bilateral transplanted region and on regions of the putamen and cerebellum using T1-weighted MRI images and merged with PET data. The ROIs were transferred to the PET images to obtain the average radioactivity within the ROIs. The bindings of [¹¹C]PK11195 and S-[¹¹C]KTP-Me were evaluated as a ratio of standardized uptake values scaled by cerebellar radioactivity. The binding potential (BPnd) of [¹¹C]PE2I was calculated using a simplified reference tissue model^{42,43} to obtain quantitative values in the transplanted region and using a Logan reference tissue model to present parametric images⁴⁴. The influx constant (K_i) of [¹⁸F]DOPA was calculated using the Patlak reference tissue model^{45,46} to obtain quantitative values in the transplanted area. The cumulative radioactivity of [¹⁸F]DOPA was scaled to that in the cerebellum to present accumulation images. An analysis of PET data was performed using PMOD software (PMOD Technologies LLC).

Video analysis. For video analysis, monkeys were moved to special cages and video recorded for 90 min before transplantation and 6, 9 and 12 months after transplantation (Extended Data Fig. 2b–e). The recorded videos were analysed with MATLAB software (MathWorks Inc.), and the pixel change of each frame (1/30 s) was quantified (Extended Data Fig. 2f, h). The total time of movements greater than a threshold (5,000 or 10,000 movements) was defined as moving time. **Monkey PD scores.** A blinded observer evaluated PD symptoms of the monkeys once a week throughout the observation periods. The following items were assessed and scored: facial expression (normal, 0; slightly reduced, 1; reduced, 2; or absent, 3), head checking movements (normal, 0; slightly reduced, 1; reduced, 2; or absent, 3), spontaneous movement (normal, 0; slightly reduced, 1; reduced, 2; or absent, 3), movement in response to stimuli (normal, 0; slightly reduced, 1; reduced, 2; or absent, 3), tremor (absent, 0; mild/not always, 1; moderate, 2; or severe, 3), posture instability (normal, 0; impaired, 1; frequent falling, 2; or no movement, 3), and gait (normal, 0; slightly reduced, 1; reduced, 2; or no walking, 3). A score of zero indicates a normal monkey, whereas a maximum score of 21 indicates an animal with severe PD symptoms.

L-DOPA test. An L-DOPA test was performed before the transplantation. Monkeys were fasted for at least 8 h and then administered 20 mg kg⁻¹ of L-DOPA (Sigma-Aldrich) and 5 mg kg⁻¹ of benserazide hydrochloride (Sigma-Aldrich) through nasogastric tubes. Video recording for 1 h was performed just before and after the administration of L-DOPA, and then monkey PD scores were evaluated.

Microarray analysis. Human fetal tissue was obtained from legally terminated embryos with the approval of the Swedish National Board of Health and Welfare in accordance with existing guidelines, including informed consent from women seeking elective abortions. Total RNA was extracted using an RNeasy Plus Mini kit, and 50 ng of total RNA was processed by an Ambion WT Expression Kit and Affymetrix GeneChip Whole-Transcript Expression Arrays (Affymetrix) according to the manufacturer's protocol. The data were analysed with GeneSpring software (Agilent Technologies). Gene expressions found to have a fold change greater than two were considered to be significant.

Reverse transcription with polymerase chain reaction (RT-PCR). The total RNA fraction was extracted using an RNeasy Mini kit (QIAGEN) and reverse-transcribed using SuperScript III First-Strand Synthesis System (Invitrogen). Quantitative PCR reactions were carried out with Power SYBR (Applied Biosystems) according to the manufacturer's instructions. The expression level of each gene was normalized to that of GAPDH using the $\Delta\Delta^{C_t}$ method. Primers used for the reactions are as follows:

CDH11 forward: ACGCAGAGGCCTACATTCTG
CDH11 reverse: CATTAAAGCTTGGCAACCCAG
CRABP1 forward: GATCCACTGCACGCAAACTC
CRABP1 reverse: GGCGCCAACGTCAGGATAAA
CRABP2 forward: ATTCAAGTGTGGCTTGC
CRABP2 reverse: GGGCTGTCAGGTTCTCTGGA
DLK1 forward: CTGCCTGCAGCACACCC
DLK1 reverse: GGTCTCGCACTTGTGAGGA
EDNRB forward: AAAGCAGAGACGGGAAGTGG
EDNRB reverse: EDNRB CTGCTGAGGTGAAGGGGAAG
HAPLN1 forward: GAGAAAGAGCCCTAGCTTC
HAPLN1 reverse: CCCAAAGAACCTCTTCACTTGTCC
HIST1H1A forward: AAGGCAACGGGTGCATCTAA
HIST1H1A reverse: GATTCCTTGTGCGCAGG
P2RX3 forward: GGCGCTGCGTGAACTA
P2RX3 reverse: ATCATGATGGCGTTCCAC
PMEL forward: GGGCTACAAAAGGGAGCCAG
PMEL reverse: GAGACCAAGAGCCAGATGGG
RTL1 forward: CAGCGAAATGCTCTGCACTC
RTL1 reverse: GGGTGAECTGACACCGAAG
ZIC1 forward: ACATGAAGGTCCACGAATCCTC
ZIC1 reverse: AGGGCGATAAGGAGCTGTG

Immunostaining. For *in vitro* studies, spheres were fixed with 4% paraformaldehyde and sectioned at 10-μm thickness using a cryostat (CM-1850; Leica Biosystems). For *in vivo* studies, animals were perfused with 100 mM PBS and then 4% paraformaldehyde in PBS under deep anaesthesia with sodium pentobarbital (100 mg kg⁻¹ intravenously). Brains were post-fixed for 1 day with 4% paraformaldehyde and then transferred to 10, 20 and 30% sucrose solution at 4 °C. The brains were sectioned at 40-μm thickness using a microtome. Double- or triple-labelled immunohistochemical analyses were carried out after permeabilization and blocking with 0.3% Triton X-100 and 5% donkey or goat serum. The immunoreactive cells were visualized using a fluorescence microscope (BZ-9000; Keyence) and a confocal laser microscope (Fluoview FV1000; Olympus). The primary antibodies used are as follows: STEM121 (Cellartis, Y40410, 1:500), Ki-67 (Novo CASTRA, NCL-Ki-67p, 1:1,000), TH (Millipore, AB152, 1:400), GIRK2 (Alomone Labs, APC-006, 1:200), MHC class II (Dako, M0775, 1:1,000), CD45 (Dako, M0701, 1:1,000), Monkey IgG (Nordic-MUBio BV, GAMON/IGG(H+L)/BIO, 1:2,000), FOXA2 (R&D, AF2400, 1:500), NURR1 (gift from KAN Research Institute, 1:1,000), PAX6 (BD Bioscience, 561462, 1:200), SOX1 (R&D, AF3369, 1:200), serotonin (Millipore, MAB352, 1:200), GABA (Sigma-Aldrich, A-1052, 1:10,000), VGLUT1 (Synaptic Systems, I35303, 1:1,000), CHAT (Millipore, AB144p, 1:1,000), GFAP (DAKO, Z0334, 1:400), and TUJ1 (Covance, MMS-435P, 1:600).

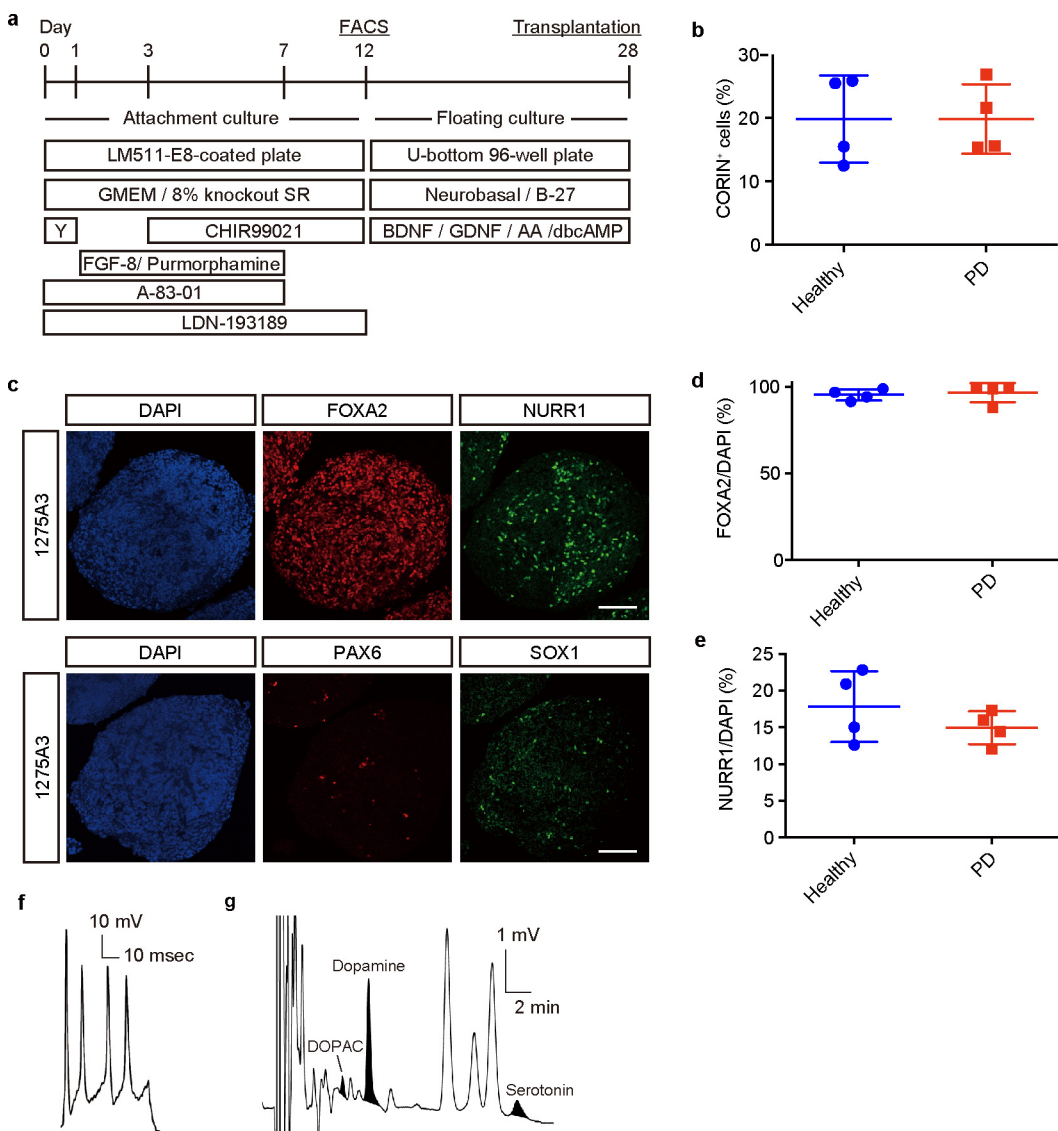
Analysis of tyrosine hydroxylase innervation. The area innervated by TH⁺ fibres was quantified from the optical density of TH immunostaining. TH⁺ fibres in caudate nuclei and putamen were detected using TH⁻ cerebral cortex as a control. For animals in the cell transplanted groups, 1 section out of 36 successive coronal sections (1 section per 1.44 mm) throughout the grafts was photographed with a microscope (BZ-X700; Keyence) and evaluated with Adobe Photoshop CC software (Adobe Systems). For animals in the vehicle group, at least two sections around needle tracts were evaluated. The percentage of innervation was calculated as the ratio of the tyrosine hydroxylase-innervated area to the whole caudate nuclei, putamen, or striatum.

Statistical analysis. The statistical analyses were performed using a commercially available software package (GraphPad Prism, GraphPad Software Inc.). Data from

in vitro analyses were compared using a *t*-test (Extended Data Fig. 1b, d, e). The behavioural data and PET data were analysed by two-way ANOVA with Dunnett's multiple comparisons test (Figs 1b, 3j, Extended Data Fig. 5a). Data from the video recordings were compared by linear regression analysis (Fig. 1c, d). Correlation of a graft size estimated from MRI and histology, and TH⁺ cells and PET or behavioural improvement were compared by a two-tailed Pearson's correlation analysis and *r* and *P* values are shown (Fig. 3l, Extended Data Figs 3b, 6a–d). Linear regression analysis was also performed, as shown in Fig. 3l and Extended Data Fig. 3b. Data from the L-DOPA test were analysed with two-tailed Wilcoxon matched-pairs signed-rank test (Extended Data Fig. 2k, l). Experimental variance was similar between study groups. Differences were considered statistically significant when *P* < 0.05, and the significance level is shown by **P* < 0.05; ***P* < 0.01; ****P* < 0.001; *****P* < 0.0001.

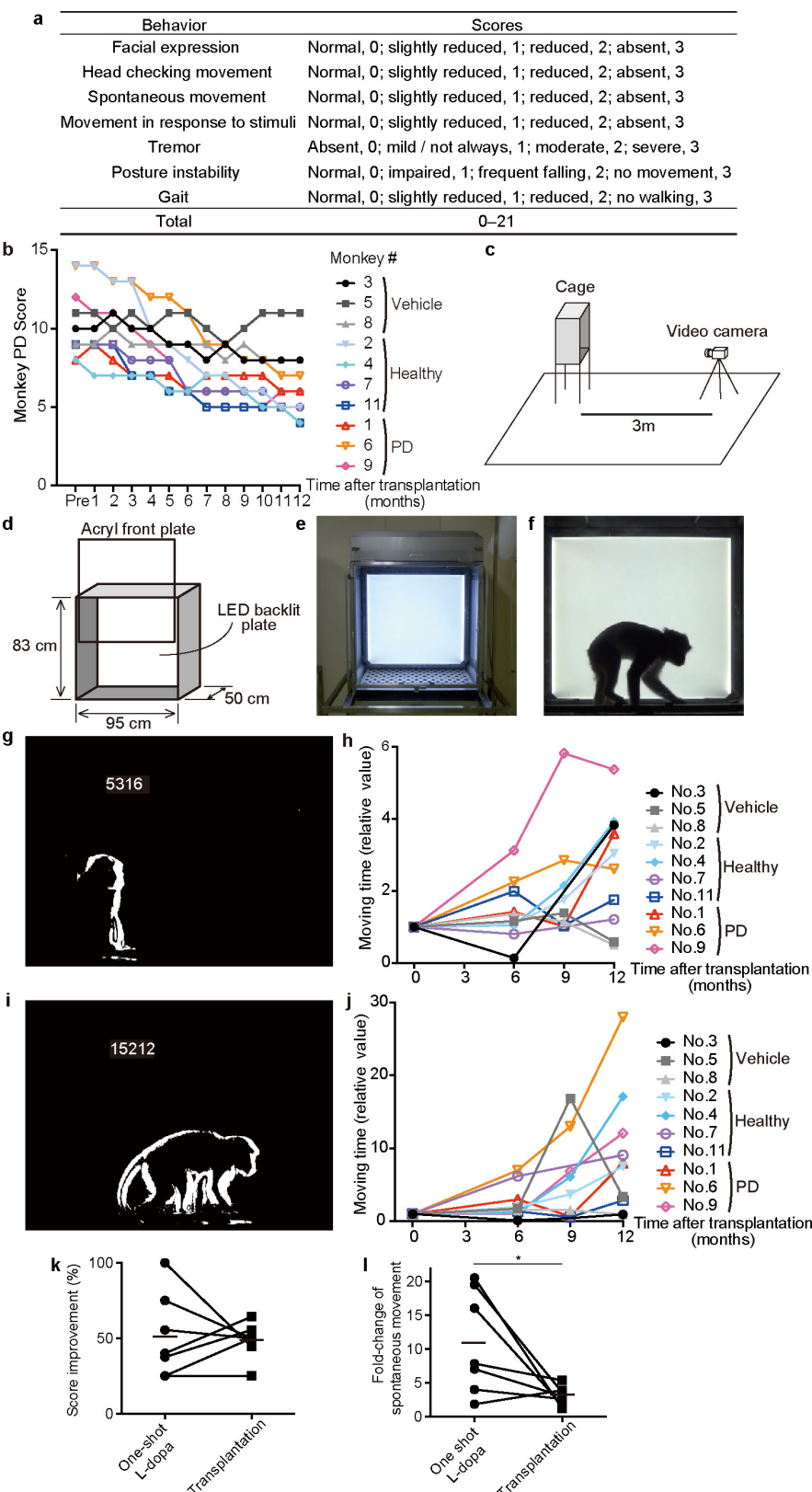
Data availability. The Source Data for Figs 1–3 and Extended Data Figs 1–3, 5–7, 9 are provided with the online version of the paper. The microarray data that support the findings of this study have been deposited in the National Center for Biotechnology Information Gene Expression Omnibus (GEO) with the accession number GSE99253.

31. Okita, K. et al. An efficient nonviral method to generate integration-free human-induced pluripotent stem cells from cord blood and peripheral blood cells. *Stem Cells* **31**, 458–466 (2013).
32. Miyazaki, T. et al. Laminin E8 fragments support efficient adhesion and expansion of dissociated human pluripotent stem cells. *Nat. Commun.* **3**, 1236 (2012).
33. Nakagawa, M. et al. A novel efficient feeder-free culture system for the derivation of human induced pluripotent stem cells. *Sci. Rep.* **4**, 3594 (2014).
34. Morizane, A., Doi, D., Kikuchi, T., Nishimura, K. & Takahashi, J. Small-molecule inhibitors of bone morphogenic protein and activin/nodal signals promote highly efficient neural induction from human pluripotent stem cells. *J. Neurosci. Res.* **89**, 117–126 (2011).
35. Smith, S. M. et al. Advances in functional and structural MR image analysis and implementation as FSL. *Neuroimage* **23** (Suppl. 1), S208–S219 (2004).
36. Smith, S. M. Fast robust automated brain extraction. *Hum. Brain Mapp.* **17**, 143–155 (2002).
37. Jenkinson, M. & Smith, S. A global optimisation method for robust affine registration of brain images. *Med. Image Anal.* **5**, 143–156 (2001).
38. Jenkinson, M., Bannister, P., Brady, M. & Smith, S. Improved optimization for the robust and accurate linear registration and motion correction of brain images. *Neuroimage* **17**, 825–841 (2002).
39. Zhang, Y., Brady, M. & Smith, S. Segmentation of brain MR images through a hidden Markov random field model and the expectation-maximization algorithm. *IEEE Trans. Med. Imaging* **20**, 45–57 (2001).
40. Frey, S. et al. An MRI based average macaque monkey stereotaxic atlas and space (MNI monkey space). *Neuroimage* **55**, 1435–1442 (2011).
41. Warschausky, S., Kay, J. B. & Kewman, D. G. Hierarchical linear modeling of FIM instrument growth curve characteristics after spinal cord injury. *Arch. Phys. Med. Rehabil.* **82**, 329–334 (2001).
42. Juicute, A., Fernell, E., Halldin, C., Forssberg, H. & Farde, L. Reduced midbrain dopamine transporter binding in male adolescents with attention-deficit/hyperactivity disorder: association between striatal dopamine markers and motor hyperactivity. *Biol. Psychiatry* **57**, 229–238 (2005).
43. Leroy, C. et al. Assessment of ¹¹C-PE2I binding to the neuronal dopamine transporter in humans with the high-spatial-resolution PET scanner HRRT. *J. Nucl. Med.* **48**, 538–546 (2007).
44. Logan, J. et al. Distribution volume ratios without blood sampling from graphical analysis of PET data. *J. Cereb. Blood Flow Metab.* **16**, 834–840 (1996).
45. Patlak, C. S. & Blasberg, R. G. Graphical evaluation of blood-to-brain transfer constants from multiple-time uptake data. Generalizations. *J. Cereb. Blood Flow Metab.* **5**, 584–590 (1985).
46. Sossi, V., Holden, J. E., de la Fuente-Fernandez, R., Ruth, T. J. & Stoessl, A. J. Effect of dopamine loss and the metabolite 3-O-methyl-[¹⁸F]fluoro-dopa on the relation between the ¹⁸F-fluorodopa tissue input uptake rate constant *K*_{occ} and the [¹⁸F]fluorodopa plasma input uptake rate constant *K*_p. *J. Cereb. Blood Flow Metab.* **23**, 301–309 (2003).



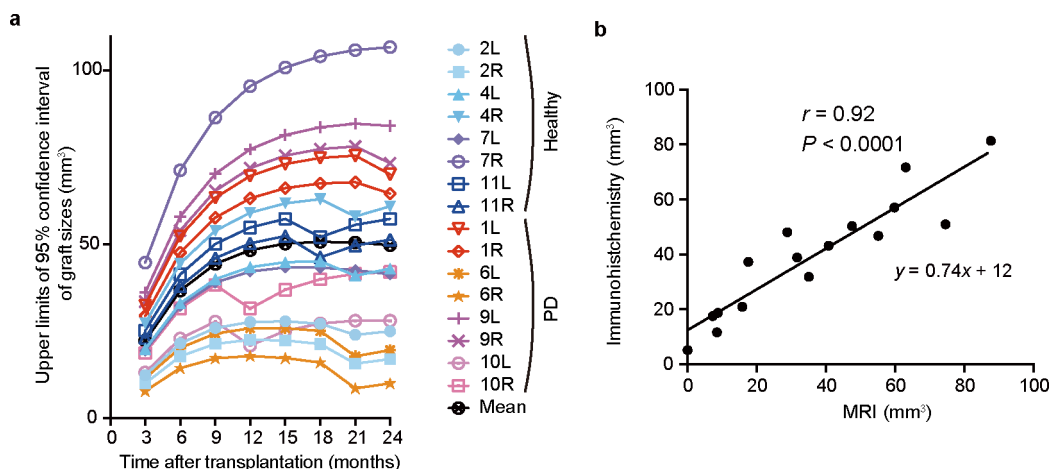
Extended Data Figure 1 | In vitro analysis of dopaminergic neuron progenitors. **a**, The protocol for the induction of dopamine neuron progenitors. Y, Y-27632; BDNF, brain-derived neurotrophic factor; GDNF, glial cell line-derived neurotrophic factor; AA, ascorbic acid; dbcAMP, dibutyryladenosine cyclic monophosphate. **b**, Percentages of CORIN⁺ cells at day 12. Values are mean \pm s.d. ($n = 4$ each for PD group and healthy group). **c**, Representative images of immunostaining for FOXA2, NURR1, TUJ1, PAX6, and SOX1 at day 26. Scale bar, 50 μ m.

d, e, Quantification of immunostaining for FOXA2 (**d**) and NURR1 (**e**) at day 26. Values are mean \pm s.d. ($n = 4$ each for PD group and healthy group). **f**, A representative current-clamp recording of the action potentials induced by brief current pulses at day 70 (1231A3). **g**, A representative chromatogram from HPLC analysis at day 42 (1231A3). DOPAC, 3,4-dihydroxyphenylacetic acid. *t*-tests were performed in **b**, **d**, and **e**. There was no significant difference between healthy and PD groups.



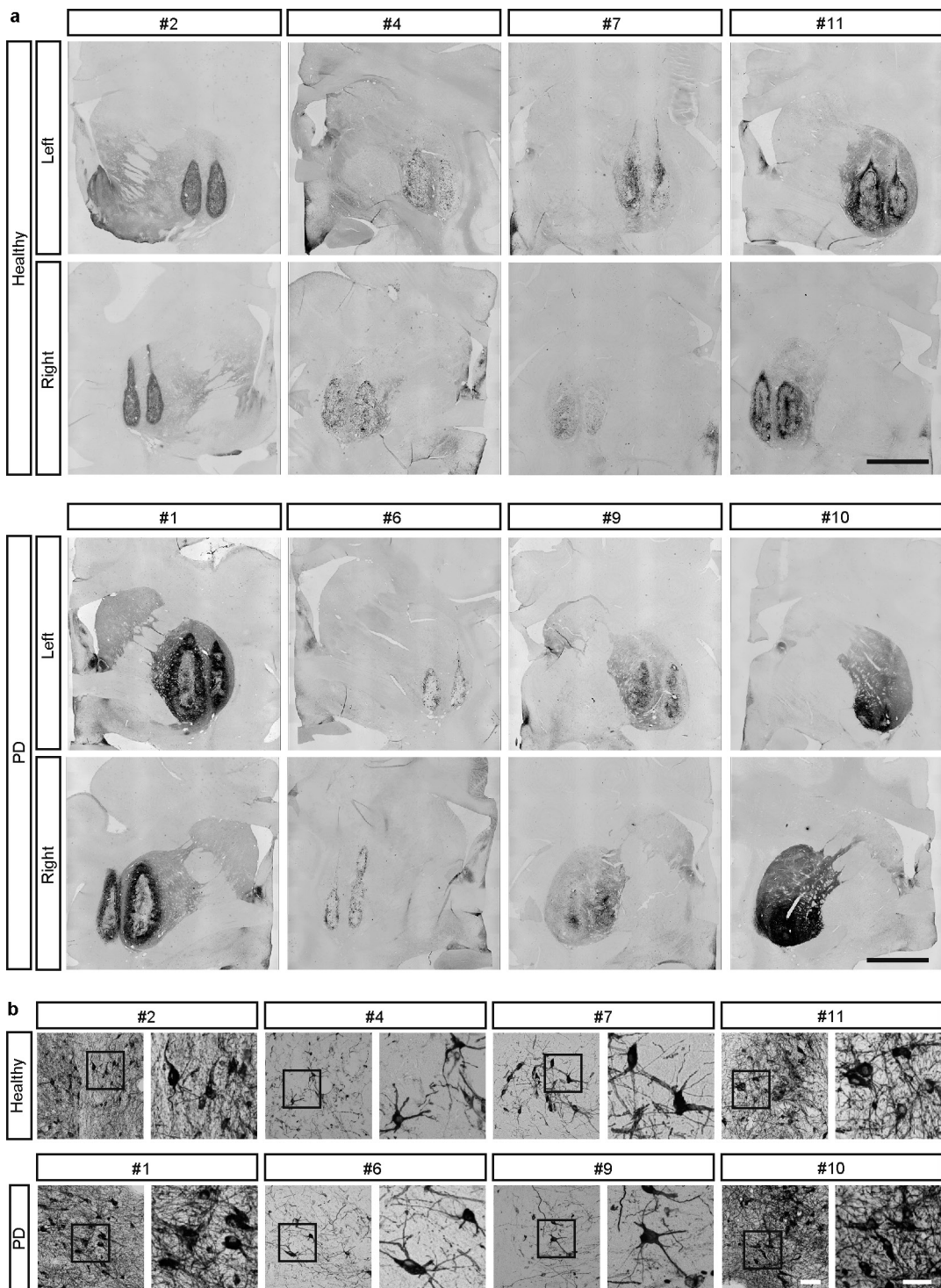
Extended Data Figure 2 | Behavioural analysis of monkeys. **a**, Rating scale of PD model monkeys. **b**, PD scores of each monkey. **c–f**, The video analysis system. Schematic view of the video recording system (**c**), simplified illustration of the special cage for the video recording (**d**), a photo of the cage with the LED backlight switched on (**e**), and a representative capture from the video recording (**f**). **g–j**, Representative captures of the video analysis when the monkey's number of movements was quantified as 5,316 (**g**) and 15,212 (**i**), and the moving time of each

monkey analysed by video recording when the threshold was set to 5,000 (**h**) or 10,000 (**j**) pixels per 0.033 seconds. In **h** and **j**, values are shown relative to each pre-operative value, which was set to 1. **k, l**, Improvement of monkey PD scores (**k**) or fold change in spontaneous movement analysed by video recording (**l**) after administration of one-shot L-DOPA or transplantation. Horizontal bars designate the mean value. Two-tailed Wilcoxon matched-pairs signed rank-test was performed. * $P < 0.05$.

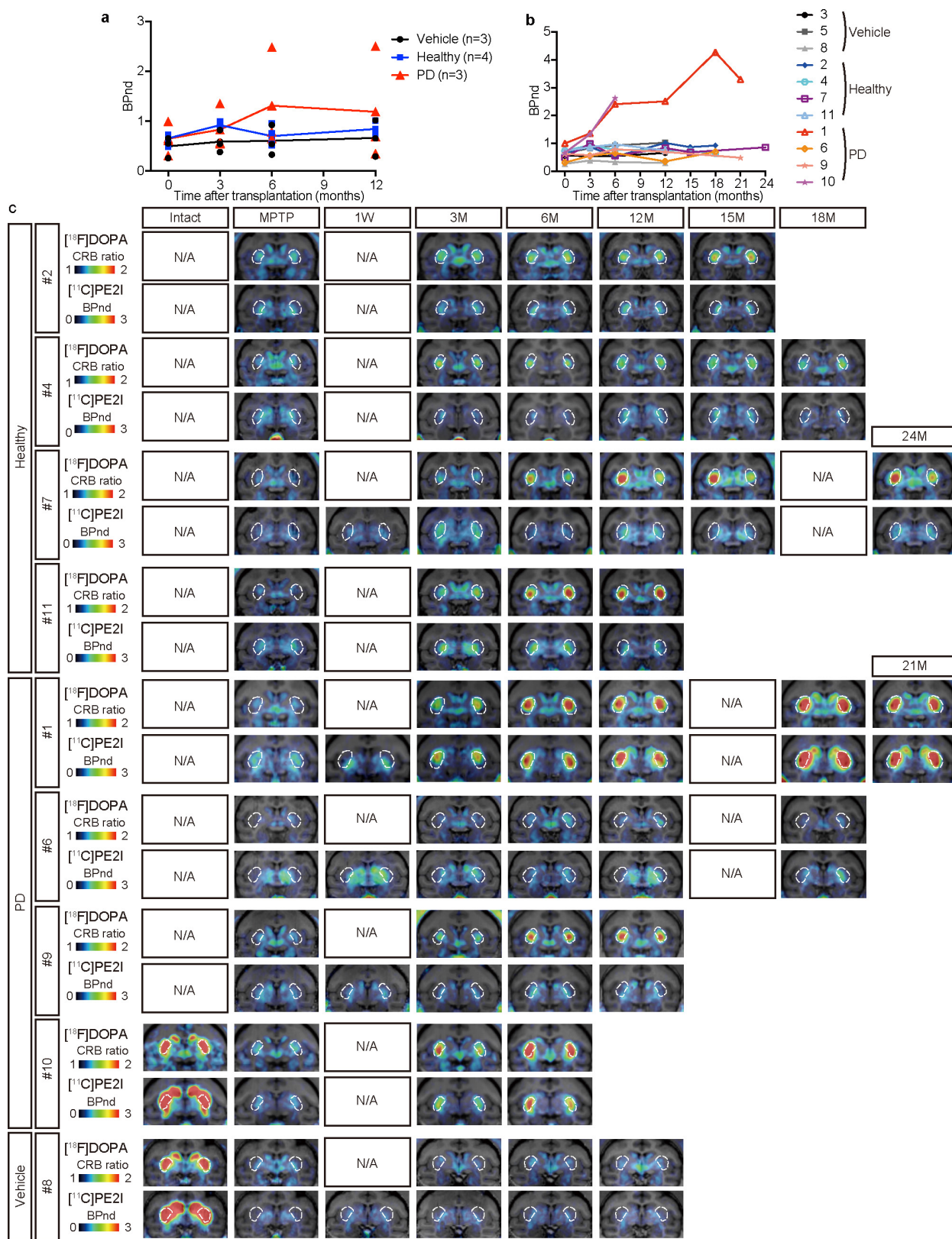


Extended Data Figure 3 | Estimation of graft growth. **a**, Estimated maximum volume of the grafts within 95% confidence upper limit analysed by a linear mixed effect model. **b**, Correlation between the graft

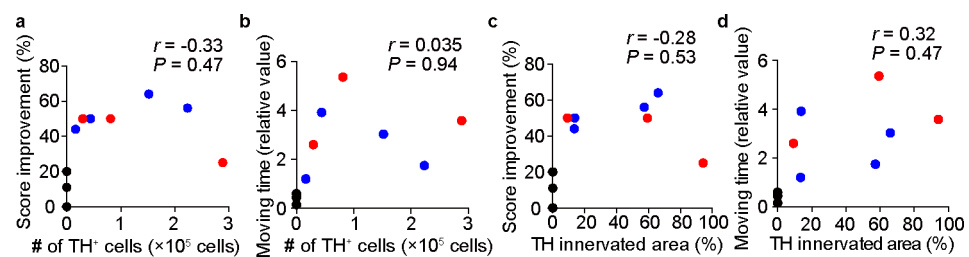
volumes calculated from MRI and measured by histological analysis ($n=16$). Data were compared using a two-tailed Pearson's correlation analysis, and r and P values and linear regression lines are shown.



Extended Data Figure 4 | Tyrosine hydroxylase histology of monkeys. **a**, Representative tyrosine hydroxylase staining of each monkey. Scale bars, 5 mm. **b**, Representative magnified view of TH⁺ cells in each graft. Scale bars, 100 μ m (left) and 50 μ m (right).

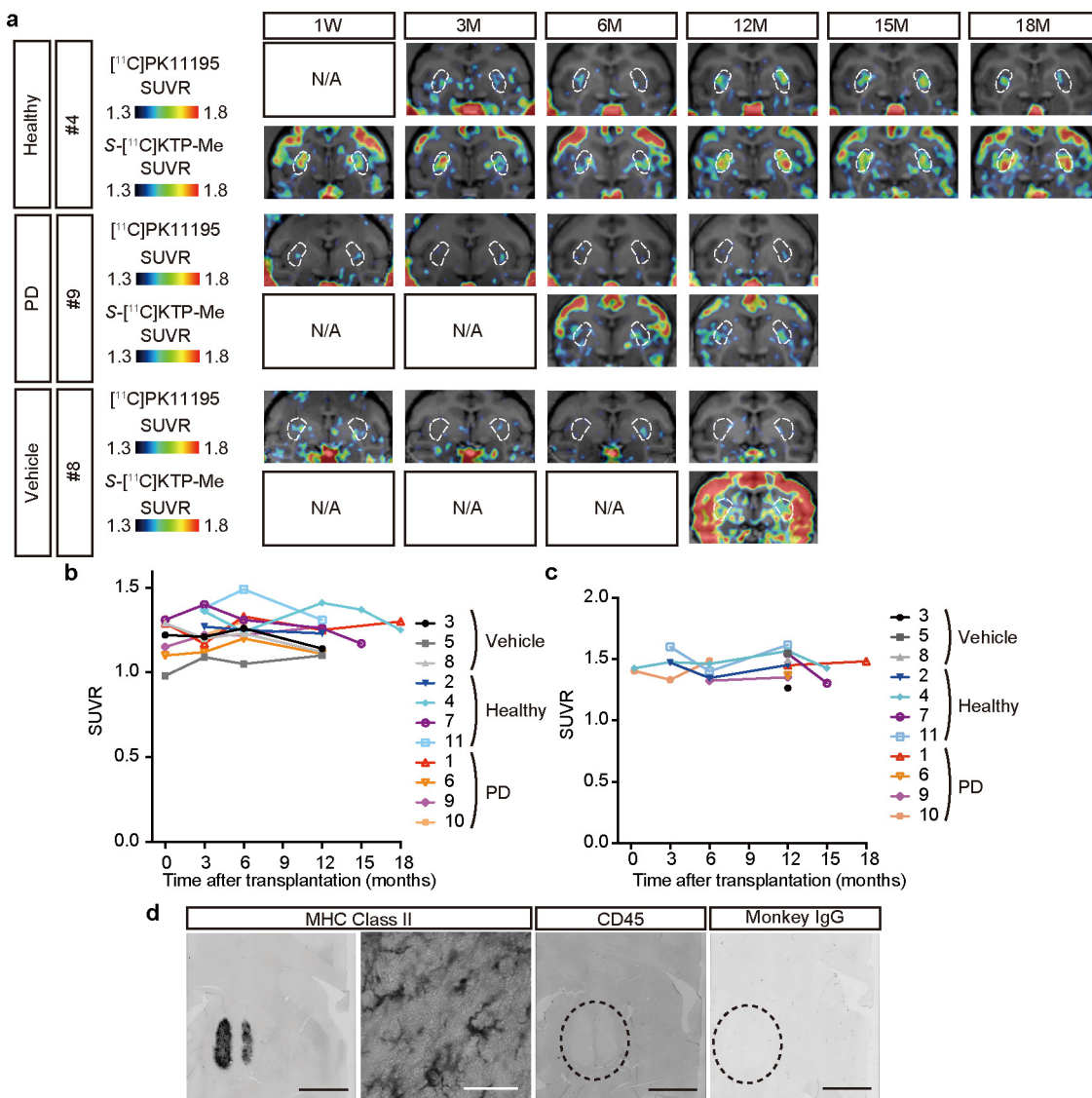


Extended Data Figure 5 | $[^{18}\text{F}]$ DOPA- and $[^{11}\text{C}]$ PE2I-PET of monkeys. **a**, Binding potential (BPnd) values of $[^{11}\text{C}]$ PE2I-PET. Lines show mean values ($n=3$ for vehicle and PD groups, 4 for healthy group). **b**, BPnd values of $[^{11}\text{C}]$ PE2I-PET in each monkey. **c**, $[^{18}\text{F}]$ DOPA- and $[^{11}\text{C}]$ PE2I-PET of each monkey. Dotted white lines designate the putamen.



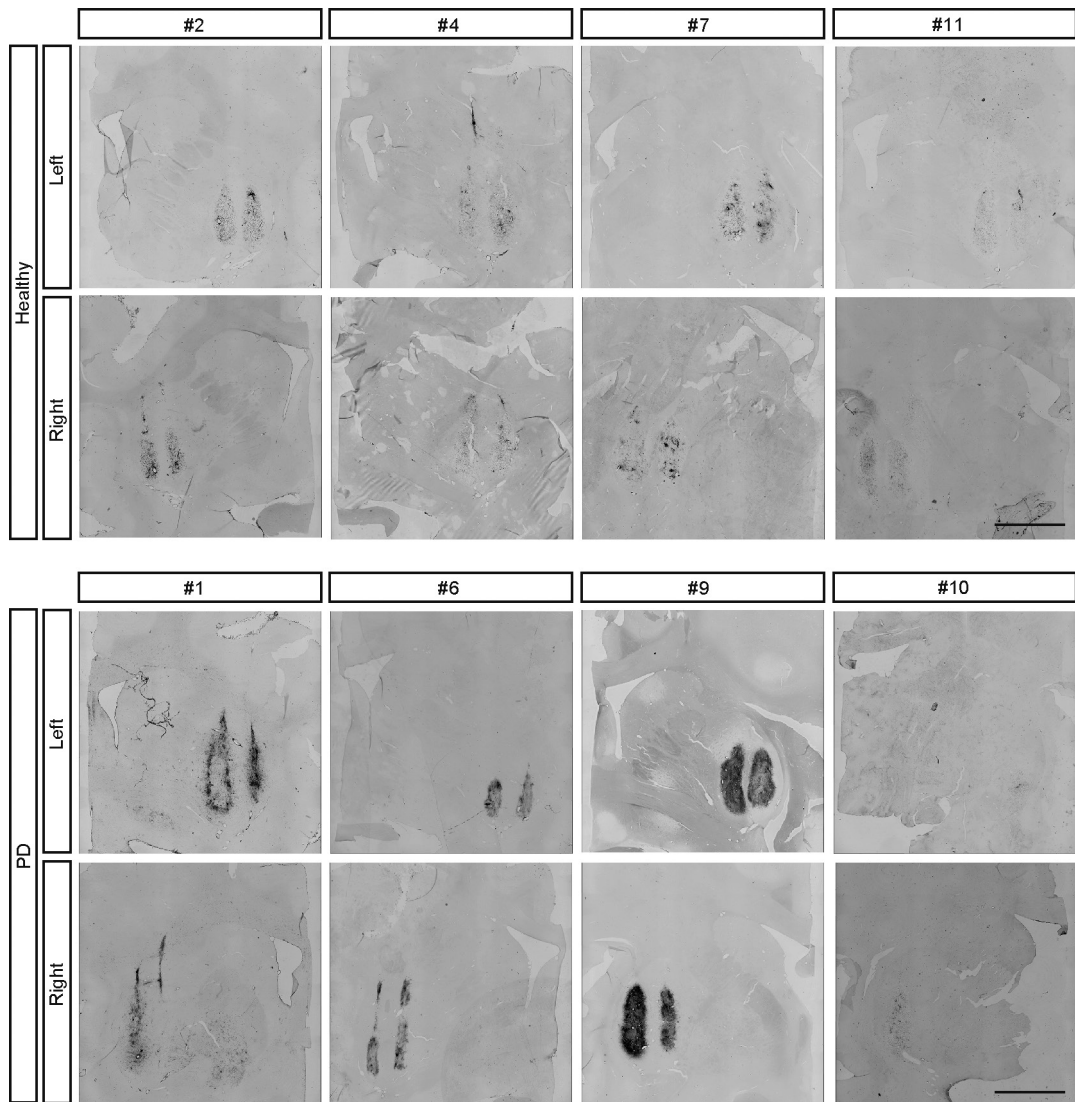
Extended Data Figure 6 | Correlation between surviving TH⁺ cells and functional recovery. **a, b,** Correlation between the number of surviving TH⁺ cells and score improvement (a) and moving time analysed from the video recording (b). **c, d,** Correlation between tyrosine hydroxylase-

innervated area and score improvement (c) and moving time (d). Two-tailed Pearson's correlation analysis was performed, and r and P values are shown. Data for the healthy group are shown in blue, the PD group in red, and the vehicle group in black.

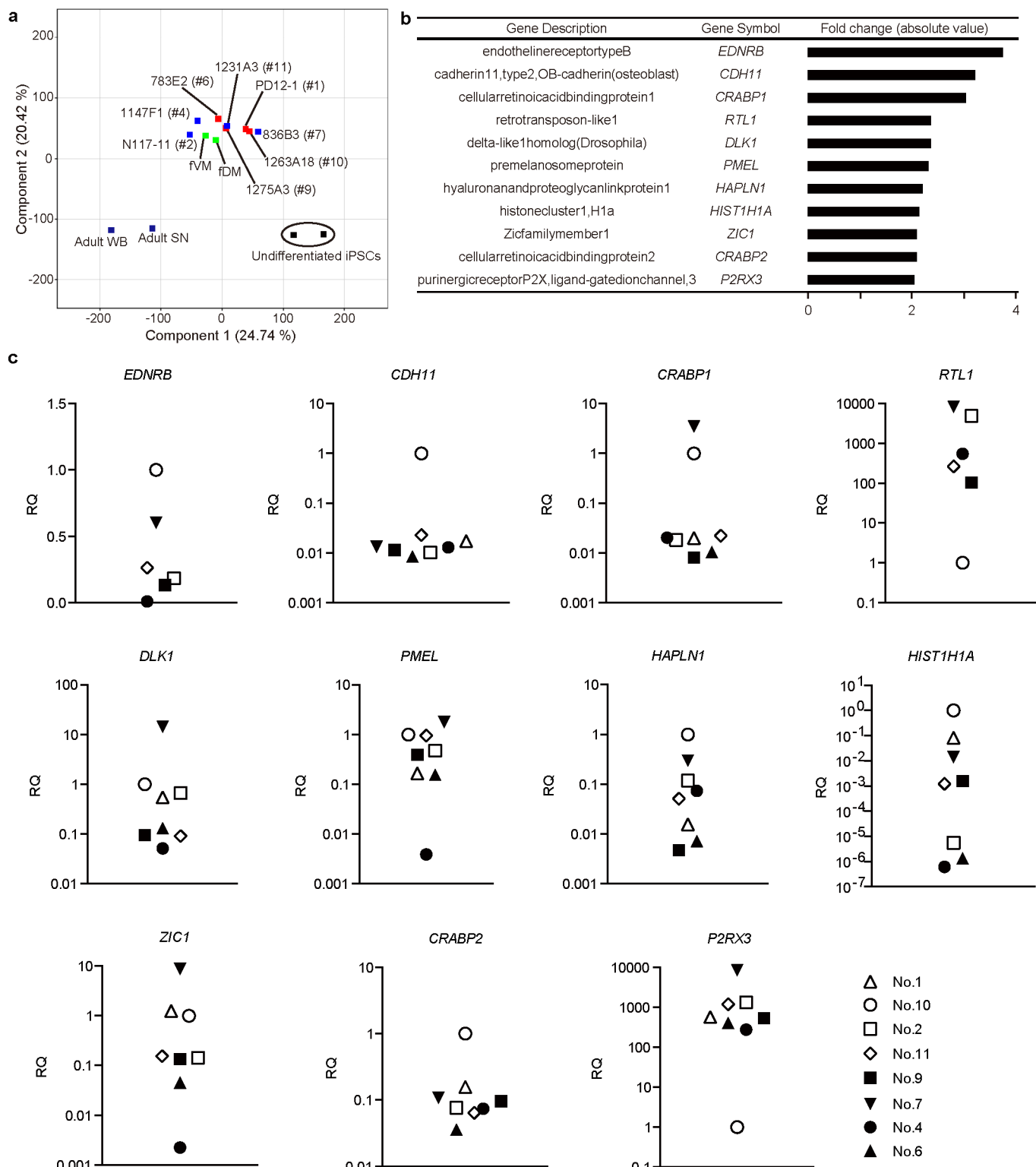


Extended Data Figure 7 | Inflammation in the brains of cell-transplanted monkeys. **a**, Uptake ratios of [¹¹C]PK11195-PET and S-[¹¹C]KTP-Me-PET in representative monkeys. Dotted white lines designate the putamen. **b, c**, Ratio of standardized uptake values of [¹¹C]PK11195-PET (**b**) and S-[¹¹C] KTP-Me-PET (**c**). **d**, Representative

images of MHC class II, CD45, and monkey IgG staining of monkey number 9. Dotted lines designate the grafted area. Scale bar, 5 mm for the left side of MHC class II, CD45, and monkey IgG, and 50 μ m for the right side of MHC class II.



Extended Data Figure 8 | Representative MHC class II staining of each monkey. Scale bars, 5 mm.



Extended Data Figure 9 | Gene expression analysis of the transplanted cells. **a**, Principal component analysis of the transplanted cells (healthy group in blue, PD group in red), two iPS cells (836B3 and 1231A3, black), fetal ventral midbrain tissue (fVM, green), fetal dorsal midbrain tissue

(fDM, green), adult whole brain tissue (WB, navy), and adult substantia nigra tissue (SN, navy). **b**, Gene list obtained from the microarray analysis. **c**, Quantitative PCR analysis of the transplanted cells. Values are expressed as relative quantity (RQ).

Extended Data Table 1 | Blood concentration of FK506 in each monkey (ng ml⁻¹)

Monkey #	3M	6M	9M	12M	15M	18M	21M	24M
3	14.0	18.8		23.0				
5	12.0	18.5		13.8				
8	9.4	17.0	32.5	27.3				
2	12.4	21.4	12.8	26.6		28.6		
4	14.0	9.2	19.9	26.6		23.6		
7	47.0	10.0	15.3	17.7		19.1		15.0
11	27.0	28.7	25.0	10.9	19.5			
1	15.0	37.0	19.0	23.6		16.6	13.9	
6	23.0	89.0	14.1	24.7		25.7		
9	11.0	16.0	18.6	28.0	16.8	25.6	29.1	
10	44.0	24.8						